ACS OMEGA

Open Access

http://pubs.acs.org/journal/acsodf

Article

Electrochemical and DFT Studies of the *Pistacia Integerrima* Gall Extract: An Eco-friendly Approach towards the Corrosion of Steel in Acidic Medium

Jasdeep Kaur, Hamad Almujibah, Mohammad Mahtab Alam, Abha Singh, Akhil Saxena,* Dakeshwar Kumar Verma, and Elyor Berdimurodov

Cite This: *ACS Omega* 2024, 9, 7643−7657

Read Online

ACCESS | Metrics & More | Article Recommendations | Supporting Information

ABSTRACT: A novel application of the *Pistacia integerrima* gall extract as an environmentally friendly corrosion inhibitor is reported in this study. The major phytochemicals present in the gall extract, namely pistagremic acid, *β*-sitosterol, pistiphloroglucinyl ether, pistaciaphenyl ester, naringenin, and 5,7-dihydroxy-2-(4-hydroxyphenyl)-2,3-dihydrochromen-4-one, play key roles in its anticorrosive behavior on steel in aggressive media. Several approaches were used to study the corrosion prevention activity of steel in 1 M H_2SO_4, including weight loss analysis, scanning electron microscopy (SEM), electrochemical impedance spectroscopy (EIS), potentiodynamic polarization (PDP), and density functional theory (DFT). At 2000 mg L^{-1}, the highest efficiency of 92.19% was observed in 1 M H_2SO_4. An SEM study was conducted to validate the surface coverage of the metal surface. DFT studies revealed several nucleophilic regions present in the phytochemicals of the inhibitor, which supported the favorable nucleophilicity. Corrosion studies have not been performed on this sample. Phytochemicals make it an effective corrosion inhibitor, and its extraction process utilizes distilled water, making it better than other inhibitors. It has been proven that the obtained values of ΔE_{Inh}^{DFT} for pistiphloroglucinyl, pistaciaphenyl ether, and naringenin organic compounds were very low, confirming the high reactivity of these corrosion inhibitors. The order of the values of ΔE_{Inh}^{DFT} is as follows: pistaciaphenyl ether > pistiphloroglucinyl ether > naringenin organic compound; this suggests that pistaciaphenyl ether is more reactive than the other compounds. In this study, *P. integerrima* gall extract emerges as a novel and highly effective corrosion resistance agent in 1 M H_2SO_4, chosen for its relevance to acid pickling and cleaning processes.

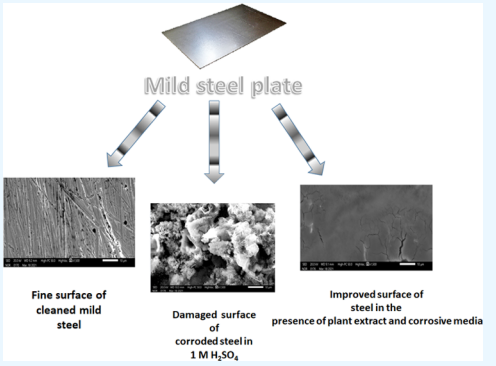

1. INTRODUCTION

The powerful mechanical strength of mild steel makes it a popular choice in many industries. However, the corrosion of mild steel happens due to the interaction between steel and aggressive materials such as H_2SO_4 and HCl, which are commonly used for pickling and descaling. Pipelines, bridges, and buildings, as well as vehicles, wastewater systems, and even home appliances, can all be damaged by corrosion.[1] A study found that iron rust absorbs arsenic easily and contaminates the environment.[2] The presence of iron rust can also speed up the growth of Legionella bacteria in water. The growth rate may be increased by 10^3−10^5 fold by ferric oxide.[3] A variety of strategies are employed to prevent corrosion, including design, material selection, and protection by electrochemical methods and inhibitor application. The application of a corrosion inhibitor is regarded as an especially cost-effective and simple method of minimizing corrosion among the listed strategies. Corrosion is controlled by a variety of chemical inhibitors, including synthetic compounds that can be harmful to humans and the environment.[2] The best way to reduce this problem is to use natural and biodegradable corrosion inhibitors that are nontoxic and affordable.[3−5]

Several plants with different phytochemicals have been reported in the literature,[6−13] which show excellent inhibition efficiency. Phytochemicals contain heteroatoms that may enhance the effectiveness of green inhibitors.[14−20] According to Bhawsar et al.,[21] *Nicotiana tabacum* extract inhibits steel in 2 M sulfuric acid with 94% efficiency at 1 g/L concentration. The alkaloids perakine and tetrahydroalastonine in *Rauwolfia macrophylla* provide corrosion protection in both HCl and H_2SO_4.[22] Applying this extract to mild steel surfaces can suppress or prevent corrosion. Various plant parts have plenty of phytochemicals that are effective corrosion inhibitors.[23−37] Plants, being ecologically friendly and plentiful, provide an affordable alternative to hazardous, chemical-based inhibitors.[38−40] In industries, there is a high probability of metals

Received: September 8, 2023
Revised: December 30, 2023
Accepted: January 22, 2024
Published: February 8, 2024

getting corroded when they come in contact with a highly corrosive environment due to acid cleaning or pickling of metal surfaces. The utility of this work is that the studied plant extract of the gall of "*Pistacia integerrima*" can be used as a pickling agent in industries wherever acidic corrosion occurs, and this reduces the corrosion rate of metal by creating a protective layer on the metal surface. This study evaluates *P. integerrima* gall extracts as eco-friendly corrosion inhibitors for steel in 1 M sulfuric acid solution using weight loss analysis, potentiodynamic polarization techniques, and electrochemical impedance spectroscopy. Following the immersion of steel samples in aggressive solutions, UV−visible spectroscopy was basically used to examine the mechanism. Additionally, scanning electron microscopy analysis was performed on steel samples to examine their surface morphology. DFT studies were also used for theoretical calculations to determine the adsorbing capacity of the phytochemicals. Kakar singhi is another name for *P. integerrima*, which belongs to the Anacardiaceae family. This plant grows at elevations between 2438 and 3657 m. *P. integerrima* is utilized as a treatment for a variety of diseases, including hepatitis, liver disorders, and inflammatory diseases, although its corrosion properties have not yet been explored. Based on the literature, the *P. integerrima* extract contains a variety of phytochemicals such as pistiphloroglucinyl, pistaciaphenyl ethers, and naringenin, which make it suitable for use as a corrosion inhibitor, and distilled water is used as a solvent for the extraction process, which in turn makes it superior to other inhibitors.

The main objective of this study is to determine the corrosion resistance capacity of the gall extract of *P. integerrima* on steel in 1 M H_2SO_4 using electrochemical methods, weight loss, and adsorption studies. Surface morphological studies are performed by scanning electron microscopy and atomic force microscopy.

2. EXPERIMENTAL STUDIES

2.1. Preparation of the Specimen of Steel. The metal (mild steel) composition employed in the research is as follows: the major component is iron (99.2%); other elements are silicon, carbon, manganese, sulfur, and phosphorus present in the proportion of 0.120, 0.105, 0.378, 0.079, and 0.0795% respectively. Steel samples have a surface area of 1 cm^2. In order to examine corrosion on steel coupons, several sandpapers were used to clean them.

2.2. Preparation of an Inhibitor from the Sample. The *P. integerrima* gall was purchased from Sirhind, Punjab. A thorough cleaning was conducted to remove dust and sand, followed by washing with double-distilled water and then drying in the shade for 3 days. The dried plant sample was then crushed to a coarse powder. Then, the crushed material (100 g) was refluxed with 250 mL of distilled water for 48 h by utilizing a Soxhlet apparatus. Afterward, the final solution was filtered to remove impurities. The extract was then dried in a hot water bath and rotatory evaporator, which was then used for further studies.

2.3. Preparation of the Corrosive Media. Loba Chemie AR grade concentrated H_2SO_4 was used to prepare 1 M H_2SO_4 in double-distilled water. We prepared solutions of different concentrations (800, 1000, 1500, and 2000 mg L^{-1}) by dissolving particular amounts of the prepared extract in 1 M H_2SO_4. In 1 M H_2SO_4, the plant extract was soluble, and the maximum solubility of the *P. integerrima* gall extract in 1 M H_2SO_4 was 2000 mg L^{-1}

2.4. Weight-Loss Measurements. For each weight loss study, 100 mL of an aggressive medium was used. A 1 cm^2 steel coupon was polished with various grades of emery paper before every corrosion study. Following weighing, the steel coupons were immersed in aggressive media of 1 M H_2SO_4 for 24 h with various inhibitor concentrations (800, 1000, 1500, and 2000 mg L^{-1}). The weight loss measurements were performed at temperatures of 298, 308, and 318 K using the following equations after the coupons were rinsed with acetone and dried:[41]

$$\eta\% = \frac{W_0 - W_i}{W_0} \times 100 \tag{1}$$

$$\theta = \frac{W_0 - W_i}{W_0}$$

$$W_0 - W_i = \Delta W \tag{2}$$

Here, ΔW represents the weight loss (gm), W_0 and W_i denote the loss of weight without the plant extract and with the involvement of the extract, respectively, and θ is the surface coverage.

2.5. Langmuir Adsorption Isotherm. The weight loss data can be applied to investigate the adsorption behavior of the extract. Equation 3 can be used to calculate the adsorption equilibrium constant[40] by plotting C/θ vs log C[7]

$$\frac{C}{\theta} = \frac{1}{K_{ads}} + C \tag{3}$$

Here, the surface coverage is denoted by θ, the extract concentration is denoted by C, and K_{ads} represents the adsorption equilibrium constant. Inhibitors are assumed to strictly follow the Langmuir adsorption isotherm if the slope of the graph and the coefficient of correlation of the straight line produced by plotting a graph of C/θ versus C are close to 1.

2.6. Analyses of Electrochemical Studies. A PGSTAT-204 Metrohm Auto lab electrochemical analyzer was used to conduct electrochemical analysis on steel coupons at 298 K.[42,43] In the corrosion cell, three electrodes were connected: the working electrode (steel), the reference electrode (calomel), and the counter electrode (platinum). A 1 cm^2 portion of the steel surface was exposed for reaction after being coated with Araldite resin. The Tafel curves were recorded in the current range of 100 nA to 1 mA in the potential range of −0.1−0.1 V. The scan rate of PDP analysis was 0.001 V/s. From the plot of the potential against the logarithm of current, the corrosion potential (E_{corr}), corrosion current (I_{corr}), and Tafel slope for the cathodic (βc) and anodic (βa) reactions were estimated.[44] Triplicate experiments were performed for each concentration to assess the reproducibility.

PDP data are used to calculate the efficiency using the following relationship[45]

$$\eta\% = \frac{I_{0corr} - I_{icorr}}{I_{0corr}} \times 100 \tag{4}$$

Here, I_{icorr} and I_{0corr} are the corrosion current density values with and without *P. integerrima* gall extract, respectively. An electrochemical workstation similar to that used for PDP analysis was used for EIS. The EIS studies were performed in the frequency range of 100,000−0.1 Hz with 10 frequencies per decade using an amplitude of 0.01 V. A 45 min immersion in an acidic medium was required to set the OCP electrode.

https://doi.org/10.1021/acsomega.3c06824
ACS Omega 2024, 9, 7643−7657

Table 1. Data of Inhibition Efficiency, Surface Coverage, and Corrosion Rate of *P. integerrima* in 1 M H_2SO_4

corrosive medium	inhibition conc. (mg L^{-1})	inhibition efficiency (%) of extract at 298 K	inhibition efficiency (%) of extract at 308 K	inhibition efficiency (%) of extract at 318 K	surface coverage (θ)	CR (mm/Y)
1 M H_2SO_4	0					396.95
	800	76.80	72.19	69.89	0.768	91.72
	1000	81.86	79.18	75.15	0.818	71.98
	1500	87.62	82.15	80.12	0.876	49.11
	2000	90.46	85.02	82.10	0.904	37.84

Equation 5 was used to evaluate the effectiveness of the inhibitor

$$\eta\% = \frac{R_{ct} - R_{ct}^{0}}{R_{ct}} \times 100 \quad (5)$$

R_{ct}^{0} and R_{ct} represent the charge-transfer resistance in the absence and presence of the plant inhibitor, respectively.

2.7. Phytochemical Testing. *The P. integerrima* aqueous extract was examined for alkaloids, flavonoids, saponins, quinones, coumarin, and sugar. 0.30 g of the concentrate was dissolved in 50 mL of distilled water, and then the solution was used for phytochemical analysis to determine which heterocyclic compounds might be present in the extract. Various tests, such as the Wagner test, Mayer test, conc. HCl test, sulfuric test, Fehling solution test, etc., were carried out as discussed below:

2.7.1. Investigation of Alkaloids. The Mayer reagent test was performed on the solution to determine its alkaloid content. A yellow color in the solution indicates the presence of alkaloids.[46]

The *P. integerrima* aqueous extract was also treated with the Wagner reagent. Brownish-reddish precipitates indicate the presence of alkaloids.[46]

2.7.2. Investigation of Flavonoids. A small amount of the *P. integerrima* aqueous extract was mixed with concentrated hydrochloric acid. A red color was a quick indicator of flavonoids.[47]

2.7.3. Investigation of Saponins. The filtrate and water were vigorously mixed. Saponins are evident by the formation of foam.[48]

2.7.4. Investigation for Quinones. In order to verify the presence of quinones, 1 mL of the extract was added to H_2SO_4, resulting in a color change.[49]

2.7.5. Test for Coumarin. 3−4 drops of alcoholic sodium hydroxide solution were mixed with the extract. A yellow coloration indicated the presence of coumarin.[49]

2.7.6. Fehling Solution Test for Sugars. Fehling solutions A and B were combined in a 1:1 ratio and boiled for 1 min. In the water bath, 1 mL of the extract was heated for 5−10 min. The presence of carbohydrates is indicated by yellowish or brick-red precipitates.

2.8. Examination for UV−Visible Spectra. An extract of *P. integerrima* in 1 M H_2SO_4 was also analyzed by using a UV−visible spectrophotometer. We conducted UV−visible analyses on solutions in which steel specimens were dipped for 24 h as well as on solutions in which steel specimens were not dipped, to examine the adsorption and desorption of the *P. integerrima* extract. It was necessary to examine both spectra to comprehend the inhibitory mechanism.[50]

2.9. Surface Inspection. The corrosion protection process was also estimated by performing SEM and AFM on steel. Specimens that were cleaned and dipped in an acid solution for 24 h without and with an inhibitor were examined through their SEM and AFM images.

2.10. DFT-Based Theoretical Investigations. Modern molecular modeling techniques, such as molecular dynamics simulations, have become powerful tools for designing and studying the mechanisms of inhibition. The importance of these calculations lies in understanding atom-scale details, the interpretation of experimental results, and the testing of corrosion inhibitors. A DFT-based theoretical investigation is performed to explore the relation between corrosion inhibition and molecular structures at the atomic scale. This is because it is difficult to gain a deep understanding of corrosion inhibition at the atomic scale by experimental investigations.[51,52] Various submethods of DFT-based theoretical studies were utilized to access the theoretical basis of corrosion inhibition by selected organic compounds.[53,54] The GAMESS-US[55] with the 6-21G basis sets,[56] density functional theory (DFT), and B3LYP[57] methods were chosen to perform the DFT-based theoretical investigations of pistiphloroglucinyl, pistaciaphenyl ether, and naringenin corrosion inhibitors. wxMacMolPlt[58] and Avogadro[59] were employed for analysis and visualization.

3. RESULTS AND DISCUSSION

3.1. Measurements of Weight Reduction. Weight loss values are recorded at temperatures of 298, 308, and 318 K, which are depicted in Table 1, at different concentrations of the *P. integerrima* gall extract, and mild steel surface coverage and inhibition efficiency were calculated. According to the information in Table 1, on moving toward higher concentrations of the inhibitor, more area of the surface is occupied by the inhibitor molecules, and the corrosion process on the steel surface is reduced as the inhibitor molecule creates a barrier by forming a protective layer on the steel surface, and hence, the corrosion inhibition efficiency increases with each inhibitor concentration.

This increase is possible only if heteroatoms with lone pairs are absorbable on the metal surface and delay the pace of metal corrosion in the abrasive medium. As the concentration of inhibitors increases, the corrosion rate declines.

3.2. Langmuir Adsorption Isotherm Study. The Langmuir adsorption study provided the theoretical description of the adsorption of the inhibitor molecule on the surface of mild steel. Here, the data obtained from the weight loss were fitted in the Langmuir adsorption isotherm, and the effectiveness of the inhibitor was observed. The graph of concentration (C) of the *P. integerrima* gall extract against C/θ is shown in Figure 1. The adsorption equilibrium constant (K_{ads}), the slope of the line, and the intercept were calculated. If the slope of the line is close to about 1, it is considered that the inhibitor adsorbs on the surface of the mild steel properly.[60]. Here, the obtained line is linear, with a slope value of 0.97848; hence, this confirms the proper adsorption of the inhibitor. The calculated value of K_{ads} was 0.0470 L/mg at a temperature of 298 K.

The obtained K_{ads} value was used to determine the standard free energy of adsorption (G_{ads}^{0}) according to eq 6

https://doi.org/10.1021/acsomega.3c06824
ACS Omega 2024, 9, 7643−7657

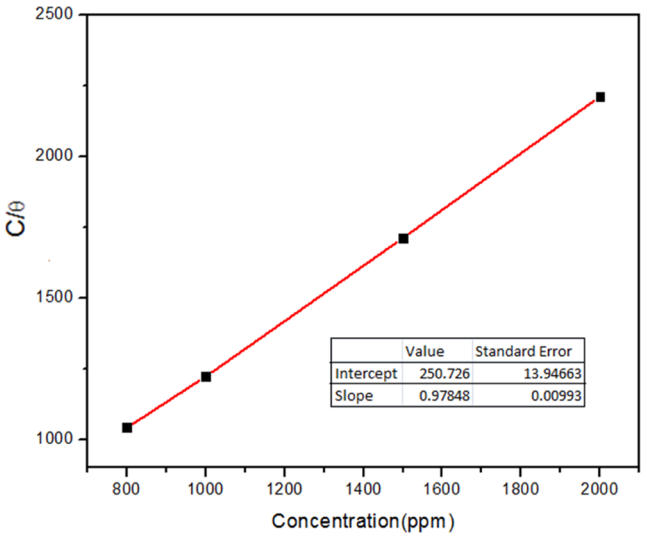

Figure 1. Adsorption isotherm study for *P. integerrima* on steel in 1 M H_2SO_4.

$$\Delta G^0_{ads} = -RT \ln (55.5 \times K_{ads}) \quad (6)$$

where ΔG^0_{ads} is the standard free energy of adsorption, the molar concentration of water = 55.5, R is the gas constant, and T is the absolute temperature.

Physisorption bonding of an inhibitor is indicated by a value of ΔG^0_{ads} equal to or more positive than −20 kJ mol^{-1}, while its chemisorption on a mild steel surface is indicated by a value equal to or more negative than −40 kJ mol^{-1}.[60] Based on eq 6, ΔG^0_{ads} is −2.37 kJ mol^{-1} at 298 K, which indicates surface physisorption on the metal. A corrosion inhibitor is considered effective due to the possibility of interaction between the above-mentioned phytochemicals and metal surfaces. Coatings prevent corrosion on mild steel surfaces by blocking the active sites.

3.2.1. Activation Parameter. As shown in Figure 2, it is possible to calculate the activation energy E_a by relating the log (CR) and 1000/T (at temperatures of 298, 308, and 318 K). The Arrhenius law states that E_a varies with temperature, which

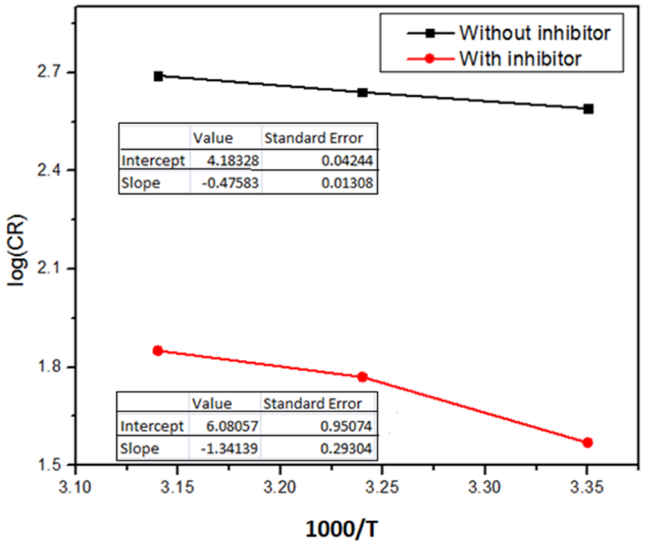

Figure 2. Plot showing the log of the corrosion rate for metal dissolutions with and without the plant extract against 1000/T.

accelerates the corrosion of metals, and E_a can be calculated according to eq 7.

$$E_a = -\text{slope} \times 2.303 \times 8.314 \quad (7)$$

On increasing the amount of the inhibitor in the corrosive solution, the activation energy values increased.[61] The calculated value of the activation energy for the blank solution (0 mg L^{-1}) is 9.09 kJ mol^{-1}; this value was increased to 50.31 kJ mol^{-1} at 2000 mg L^{-1} inhibitor concentration.

3.2.2. Adsorption Parameters. Adsorption entropy and enthalpy were calculated using the following equation

$$\log\left\{\frac{CR}{T}\right\} = \log\left\{\frac{R}{N_a h}\right\} + \frac{\Delta S_a}{2.303R} - \frac{\Delta H_a}{2.303\,RT} \quad (8)$$

In this formula, N_a, h, ΔS_a, and ΔH_a represent the Avogadro number, Planck constant, standard activation entropy, and standard activation enthalpy, respectively.

As illustrated in Figure 3, a graph of log (CR/T) against 1000/T is plotted to determine the ΔH_a and ΔS_a parameters shown in

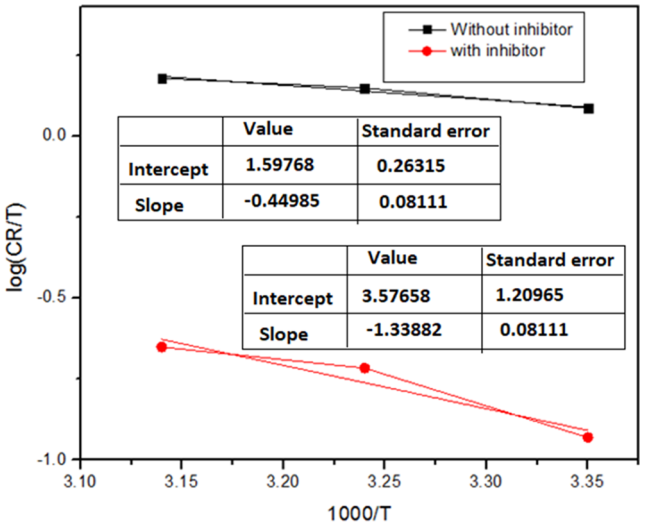

Figure 3. Graph of log (CR/T) versus 1000/T regarding the dissolution of the metal both without and with the gall extract.

Table 2. Different Parameters for Steel Both in the Presence and in the Absence of the Gall Extract in 1 M H_2SO_4

plant extract	extract concentration in (mg L^{-1})	ΔH_a (kJ mol^{-1})	ΔS_a (J mol^{-1} K^{-1})
P. integerrima gall extract	0	8.59	20.12
	2000	25.46	58.03

Table 2. As a result of the corrosion-preventing energy barrier maintained by the inhibitor, the metal is very well protected, as demonstrated by the fact that ΔH_a is higher when the inhibitor is present (25.46 kJ mol^{-1}) compared to that when the inhibitor is not present (8.59 kJ mol^{-1}). The adsorption of the plant inhibitor increases the enthalpy of the corrosion reaction. An entropy value of 58.03 J $mol^{-1}K^{-1}$ was obtained with the inhibitor as compared to 20.12 J $mol^{-1}K^{-1}$ with the blank.

3.3. Electrochemical Studies. *3.3.1. Potentiodynamic Polarization Study (PDP).* In the aggressive solvent with

https://doi.org/10.1021/acsomega.3c06824
ACS Omega 2024, 9, 7643−7657

different extract concentrations, Figure 4 shows the cathodic as well as anodic polarization study of mild steel coupons, and

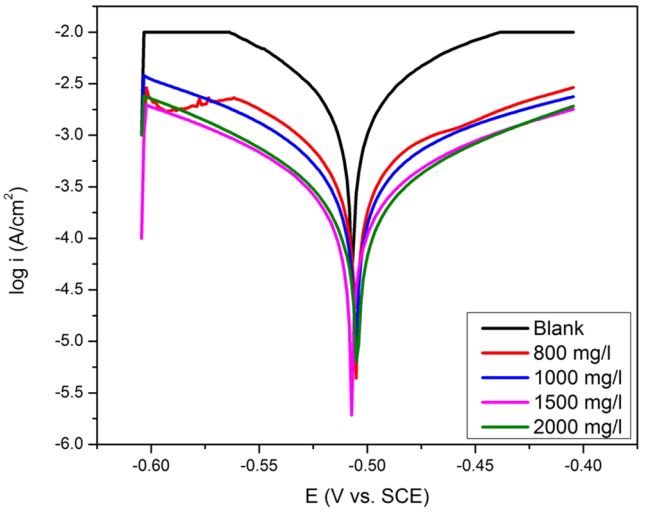

Figure 4. Tafel polarization curves in 1 M H_2SO_4 in the absence and presence of the gall extract.

Table 3 presents the related corrosion measurements and inhibition efficiencies at 298 K. Using the PDP study, the values of the corrosion current density (I_{corr}) and the corrosion potential (E_{corr}) are calculated by extrapolating the linear parts of cathodic and anodic curves. The cathodic and anodic sections of current density decrease in the presence of the *P. integerrima* extract according to the Tafel curves. This behavior demonstrates that the inhibitor may stop cathodic H_2 gas formation as well as metal oxidation.[62] Tafel graphs of the anodic and cathodic reactions changed with certain concentrations of the *P. integerrima* extract, demonstrating that the inhibitor affects the cathode H_2 gas evolution and interferes with the Fe-dissolving process. Consequently, the *P. integerrima* extract prevents cathodic and anodic corrosion reactions in 1 M H_2SO_4. As a result, adding more *P. integerrima* extract should prevent mild steel corrosion.[63] The *P. integerrima* extract concentration reduces the corrosion current density, as shown in Table 3. The calculated value of the corrosion current density for the blank solution (0 mg L^{-1}) is 2.9×10^{-3} A/cm^2; this value increased for each increase in the concentration of the inhibitor, and at the final concentration, i.e., at a concentration of 2000 mg L^{-1}, its value was 2.7×10^{-3} A/cm^2. Accordingly, we conclude that the values of inhibition efficiency increase with increasing inhibitor concentration. The highest inhibition efficiency was observed to be 90.68%. A decline in the corrosion rate (CR) is also shown in Table 3. This can be attributed to the extract adsorbing onto the surface of the metal, which reduces metal dissolution through the formation of a protective layer.

3.3.2. Electrochemical Impedance Spectroscopy Study. The Nyquist and Bode diagrams are shown in Figure 5a,b, and

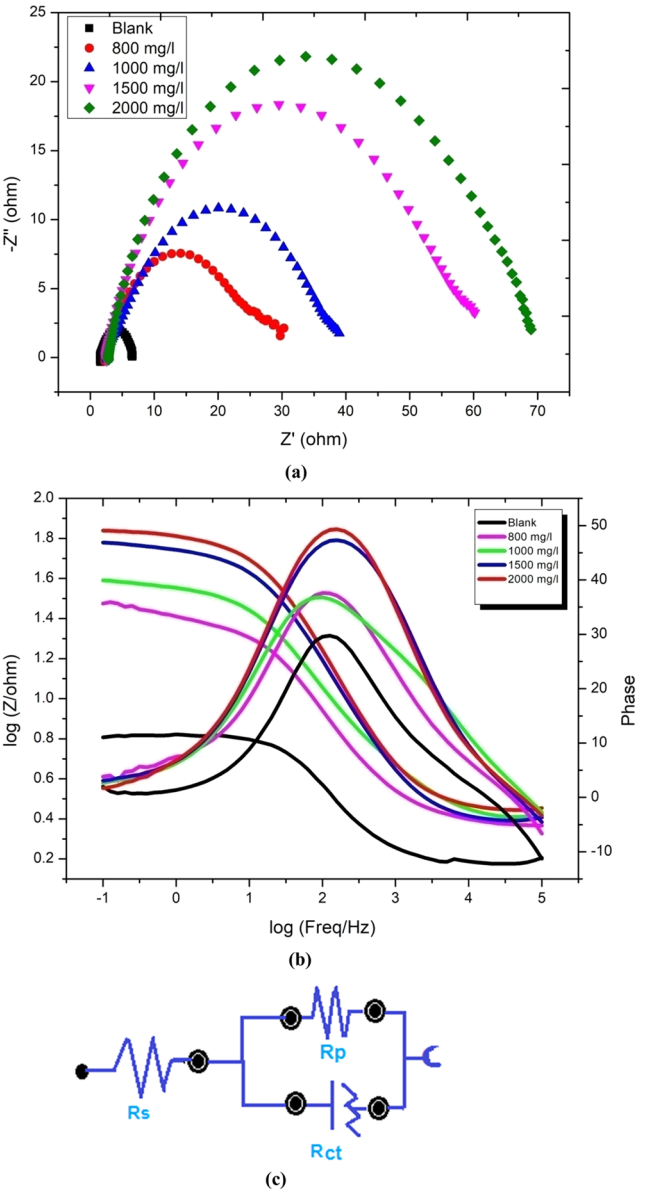

Figure 5. Nyquist (a) and Bode (b) plots and the constant phase element circuit (c) for steel in 1 M H_2SO_4 with and without the *P. integerrima* extract at 298 K.

the results are depicted in Table 4. Figure 5c represents the circuit used in this study. It is clear from Figure 5a that the diameter of the capacitive loops increased when the extract was present as compared to when the extract was not added, indicating that this addition of the inhibitor significantly

Table 3. Polarization Parameters Both with and without the Gall Extract at Various Concentrations

extract concentration (mg L^{-1})	E_{corr} (V vs SCE)	I_{corr} (A cm^{-2})	β_a (V/dec)	$-\beta_c$ (V/dec)	corrosion rate	efficiency (η %)
0	−0.506	2.9×10^{-3}	0.09527	0.06263	34.03	0
800	−0.696	6.37×10^{-4}	0.1582	0.0916	7.40	78.03
1000	−0.547	3.59×10^{-4}	0.0996	0.07838	4.18	87.62
1500	−0.525	3.0×10^{-4}	0.1291	0.1084	3.49	89.65
2000	−0.526	2.7×10^{-3}	0.1200	0.0973	3.23	90.68

https://doi.org/10.1021/acsomega.3c06824
ACS Omega 2024, 9, 7643−7657

Table 4. Polarization Measurements for Steel in 1 M H_2SO_4 with and without a Plant Extract

acid solution used in study	concentration of inhibitor (mg L^{-1})	R_s (solution resistance) (Ω)	R_{ct} (charge transfer resistance) (Ω)	constant phase element (CPE) (μFcm^{-2})	n	efficiency (%)
1 M H_2SO_4	0	1.482	5.22	5.19×10^{-4}	0.83	
	800	2.415	24.32	2.76×10^{-4}	0.71	78.53
	1000	2.545	36.09	2.34×10^{-4}	0.68	85.53
	1500	2.451	56.92	1.53×10^{-4}	0.72	90.82
	2000	2.850	66.87	1.30×10^{-4}	0.73	92.19

decreased the dissolution of mild steel. The deviation of the semicircles obtained in the Nyquist plot is because of corrosion-induced inhomogeneity and roughness of the working electrode (steel). In the circuit obtained by fitting the EIS data, the parameters of solution resistance (R_s), constant phase element (CPE), and charge-transfer resistance (R_{ct}) were considered. CPE can be introduced to compensate for the inhomogeneity and surface roughness of the working electrode. The outcomes shown in Table 4 indicate that increasing the amount of inhibitor will increase the value of R_{ct} as well as the inhibition efficiency.

Based on the Bode angle diagram, the presence of a protective layer on the surface just after the introduction of the inhibitor causes the curves to widen and move to the left (toward lower frequencies). This study, in particular, found that R_{ct} values increase with an increase in inhibitor concentrations, which indicates that the extract from *P. integerrima* is easily absorbable on the surface of mild steel with the highest efficiency of 92.19% at 2000 mg L^{-1} and at 298 K. The slightly flattened semicircles are an indication of nonideal capacitors caused by electrode flaws and/or surface reactions. Variations in the capacitor behavior are represented by values of $0 < n < 1$ ($n = 1$ represents a pure capacitor). In this study, n was found to be around 0.8, as shown in Table 4.[60]

3.4. Analyses of Phytochemicals. Plants are reservoirs of phytochemicals. Various tests were performed to confirm the existence of different phytochemicals in the *P. integerrima* gall extract, which helped understand the relation between the plant extract and the corrosion inhibition efficiency of the gall extract. The higher the extent of phytochemicals, the greater the efficiency of that plant.

The phytochemicals present in the *P. integerrima* extract are presented in Table 5.

Table 5. Phytochemical-Related Outcomes of *Pistacia integerrima*

S. No.	phytochemicals tested	various tests performed	results
1.	alkaloids	Wagner's test	++
		Mayer's Test	++
2.	flavonoids	Conc. HCl test	−−
3.	quinones	Concentrated H_2SO_4 test	++
4.	coumarins	Alcoholic sodium hydroxide test	++
5.	sugar	Fehling solutions test	−−
6.	saponins	Froth test	++

Based on the phytochemical analysis of the *P. integerrima* gall extract, it is clear that phytochemicals such as alkaloids, quinones, coumarin, and saponins are present, while flavonoids and sugar were reported to be absent. Therefore, alkaloids, quinones, coumarin, and saponins are the key phytochemicals that will be majorly adsorbed on the mild steel surface by forming a coordinate with the metal surface.

3.5. UV−Visible Spectroscopy. The UV spectra of the 1 M H_2SO_4 corrosive solutions at 2000 mg L^{-1} inhibitor concentration were obtained in two different experimental conditions. First of all, we recorded the UV spectra for 1 M H_2SO_4 at 2000 mg L^{-1} without dipping the mild steel coupons. Second, we immersed the steel coupon in the same solution for a time period of 24 h. Then, both of these UV spectra were compared to analyze their absorbance values. The UV spectra after dipping the mild steel coupons in the corrosive solution (after the corrosion test) showed lower values of absorbance than the spectra of the uninhibited solution before the corrosion test, as shown in Figure 6. This is because of the adsorption of

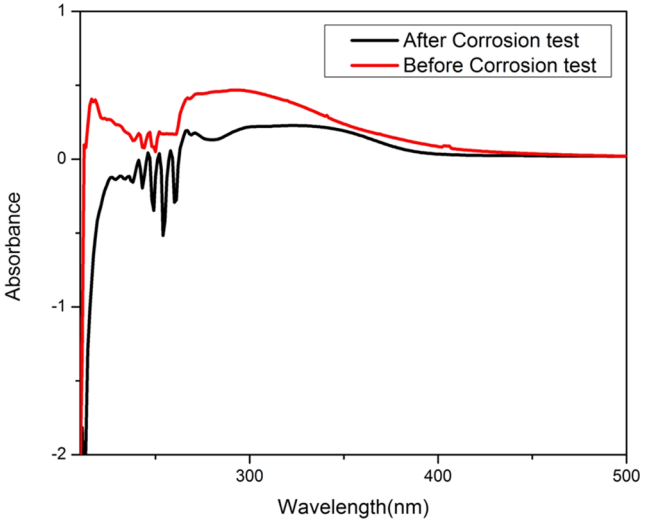

Figure 6. UV Spectrum of the solution both before and after corrosion inhibition.

the active constituents of the *P. integerrima* gall extract on the surface of mild steel, which yields lower values of absorbance. This clearly indicates the formation of a protective coating on the metal surface.[64]

3.6. Surface Examination. *3.6.1. Scanning Electron Microscopy (SEM).* Using a scanning electron microscope, the surface morphology of the mild steel coupons was determined. Here, the SEM micrographs of the coupons were obtained under three different conditions. First of all, the SEM image of the cleaned steel surface appeared to be absolutely fine, as shown in Figure 7a. Second, the same steel coupon was immersed in 1 M H_2SO_4 without the inhibitor for 24 h. Then, the SEM image was obtained and compared to the SEM image in Figure 7a. Now, the SEM image shows a highly damaged surface; this is because of the acidic corrosion taking place on the metal surface. At last, the steel coupons were dipped in 1 M H_2SO_4 with 2000 mg L^{-1} of the *P. integerrima* gall extract. Figure 7c shows that there is a significant improvement in the surface morphology of the steel. This is because of the adsorption of the *P. integerrima* gall extract

https://doi.org/10.1021/acsomega.3c06824
ACS Omega 2024, 9, 7643−7657

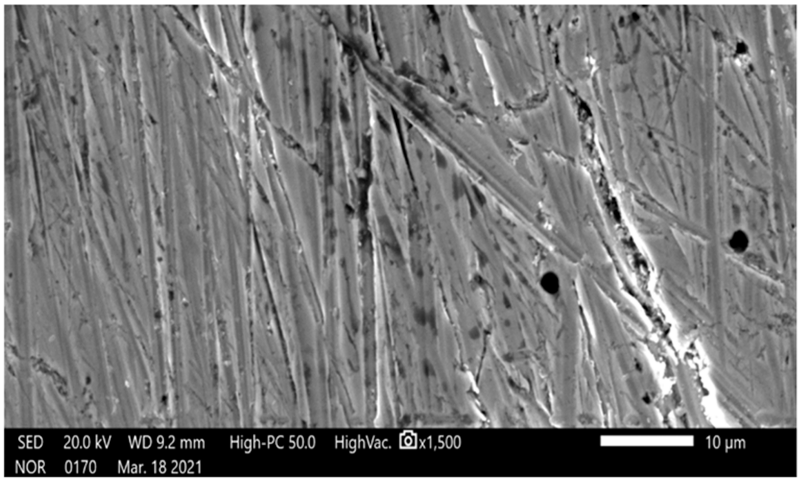

(a)

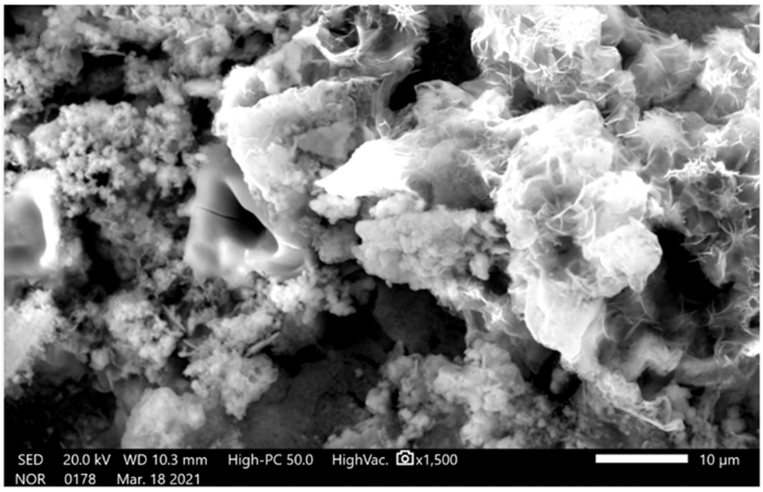

(b)

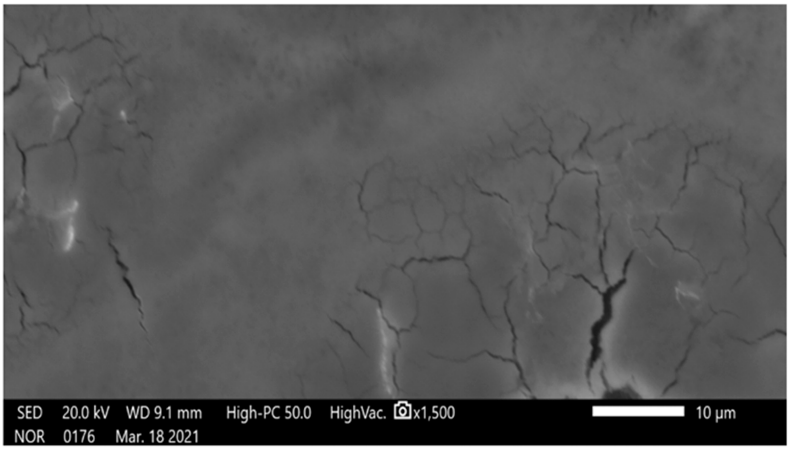

(c)

Figure 7. Images of the surface of the (a) cleaned mild steel coupon, (b) steel coupon corroded in 1 M H_2SO_4, and (c) steel coupon inhibited by 2000 mg L^{-1} extract.

on the metal surface, which forms a protective layer, creates a barrier to the acid attack, and reduces the corrosion rate.[65,66]

3.6.2. Atomic Force Microscopy (AFM). AFM images of cleaned, uninhibited, and protected steel in 1 M H_2SO_4 with the *P. integerrima* gall extract are shown in Figure 8a−c. A polished and cleaned steel surface had a roughness value of 2.08 nm. Because steel was dissolved in the acidic solution without the *P. integerrima* gall extract, its surface was extensively corroded, and its average surface roughness was recorded at 145.75 nm in this condition. The surface roughness was 25.67 nm when the *P.*

https://doi.org/10.1021/acsomega.3c06824
ACS Omega 2024, 9, 7643−7657

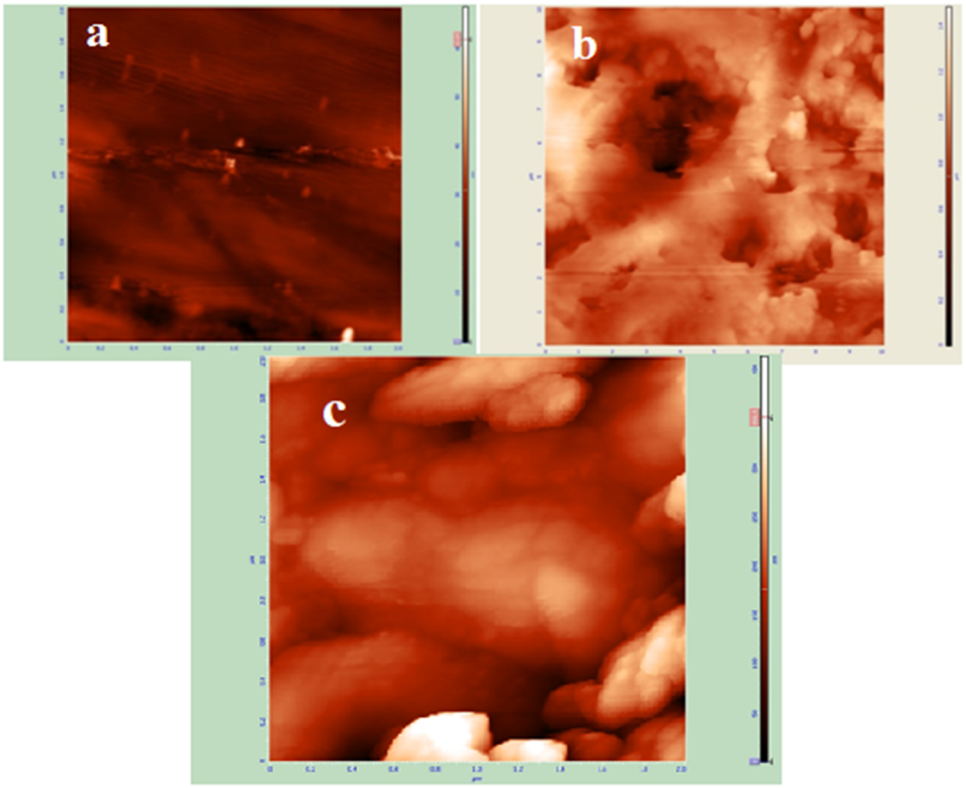

Figure 8. AFM images of (a) cleaned mild steel coupon, (b) steel coupon corroded in 1 M H_2SO_4, and (c) steel coupon inhibited by 2000 mg L^{-1} extract.

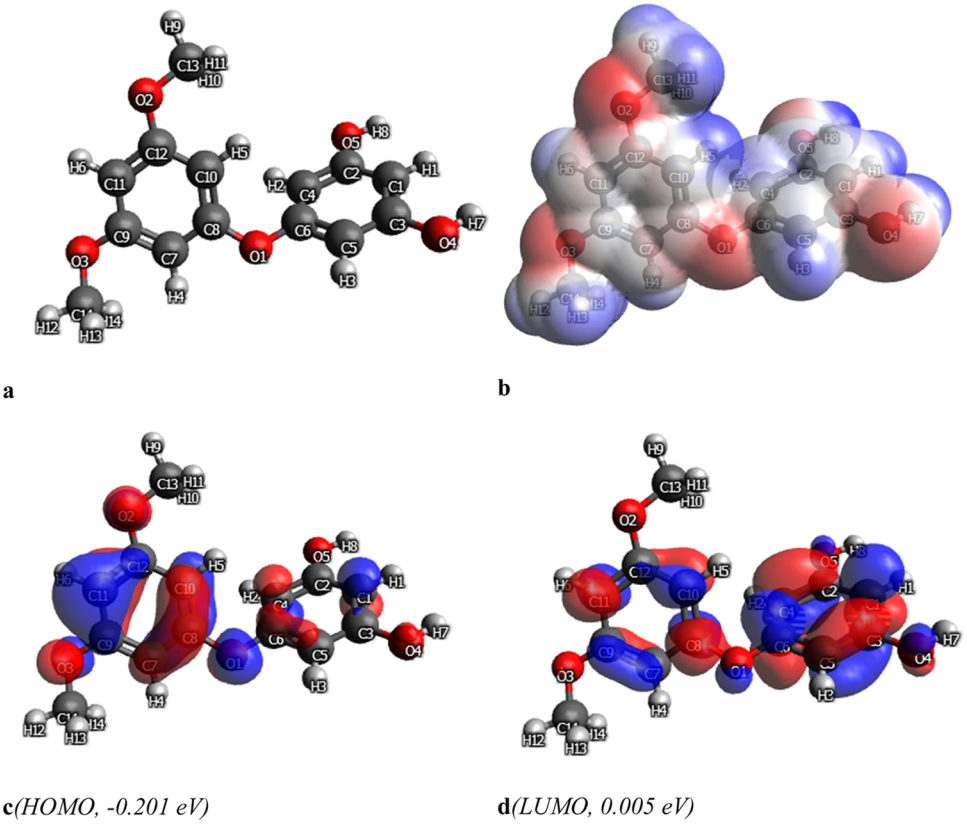

Figure 9. (a) Optimized structure and (b) MEP, (c) HOMO, and (d) LUMO structures of pistiphloroglucinyl ether.

https://doi.org/10.1021/acsomega.3c06824
ACS Omega 2024, 9, 7643−7657

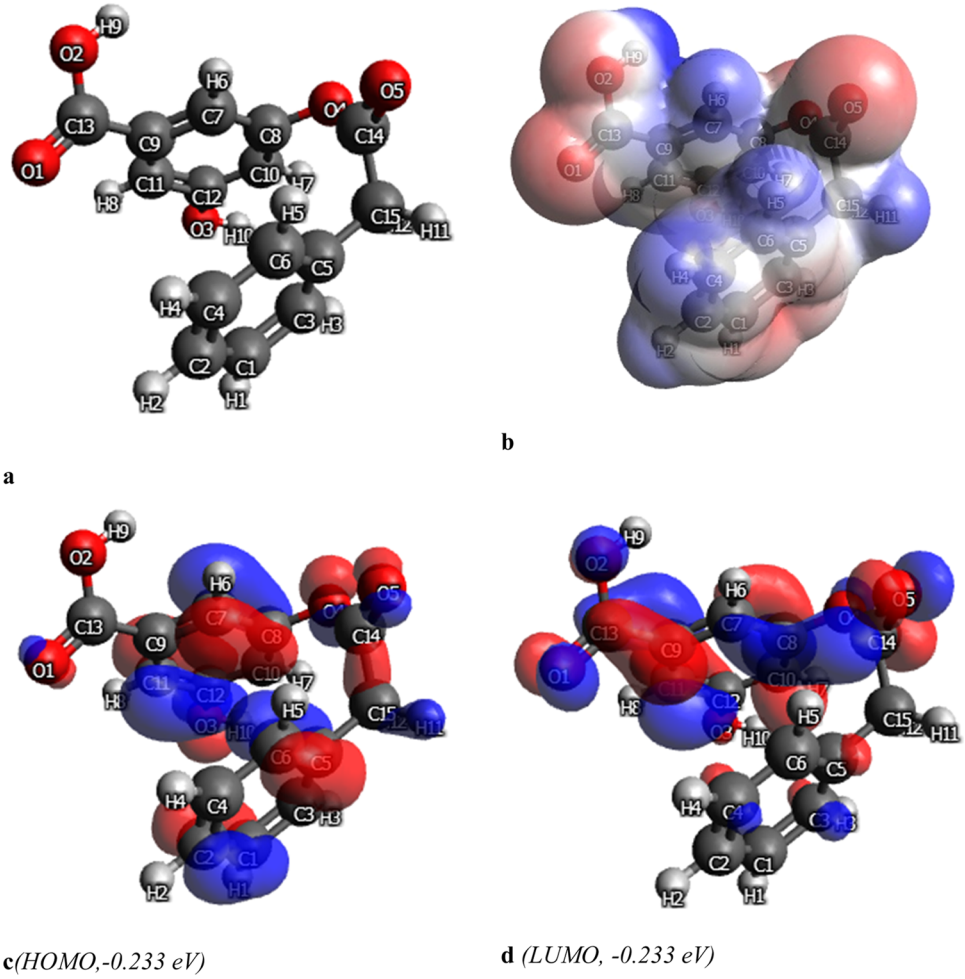

Figure 10. (a) Optimized structure and (b) MEP, (c) HOMO, and (d) LUMO structures of pistaciaphenyl ester.

integerrima gall extract was used. As can be seen from the roughening values, the metal surface has developed a protective layer.

3.7. DFT-Based Theoretical Investigations. *3.7.1. Optimization Investigations.* The corrosion inhibition effectiveness of pistiphloroglucinyl, pistaciaphenyl ether, and narengenin corrosion inhibitors depends on their nature of optimization. In this research work, the optimization analysis of the selected corrosion was performed based on the DFT calculations. The resulting optimized structures of pistiphloroglucinyl, pistaciaphenyl ether, and naringenin organic compounds are represented in Figures 9a, 10a, and 11a, respectively. Overall, what is remarkable about the findings is that the optimized structures of pistiphloroglucinyl, pistaciaphenyl ether, and narengenin corrosion inhibitors show highly polarized molecules. The values of the polarization index were also very high for all selected compounds. These results confirmed the following:

(i) The pistiphloroglucinyl, pistaciaphenyl ether, and naringenin corrosion inhibitors have a high polarization index.

(ii) Their highly polar nature promotes their good solubility in aquatic solutions.

(iii) The adsorption performance of the studied corrosion inhibitors is supported by their highly polar nature.

(iv) The benzoyl rings are polar centers in the optimized structures of pistiphloroglucinyl, pistaciaphenyl ether, and naringenin corrosion inhibitors.

(v) The oxygen of the hydroxyl functional groups and heteroatoms of the ether group promote an increase in the polarization index of the obtained molecular structures.

(vi) The transfer of delocalized π-electrons between the benzoyl rings and nonequivalent positions of active functional groups is also an additional factor for the high polarity.

3.7.2. Charge Distribution Investigations. The charge distribution is the next part of the DFT-based theoretical investigations. As observed, the charge values of the elements changed slowly. The theoretical charge values of elements were simultaneously changed in the molecular structures due to various effects, such as the stereochemical, chemical, physical, or planar nature of functional groups, heteroatoms, and the π-system. Additionally, it has been discovered that hydroxyl oxygen atoms have a stronger negative charge than others, confirming that the pistiphloroglucinyl, pistaciaphenyl ether, and naringenin inhibitors adsorbed on the steel coupons by the more negative oxygen atoms as adsorption centers.[67−69]

3.7.3. Investigations of the Molecular Electrostatic Potential (MEP). The MEP analysis shows available electrophilic and nucleophilic areas.[70−72] The resulting MEPs of pistiphlor-

https://doi.org/10.1021/acsomega.3c06824
ACS Omega 2024, 9, 7643−7657

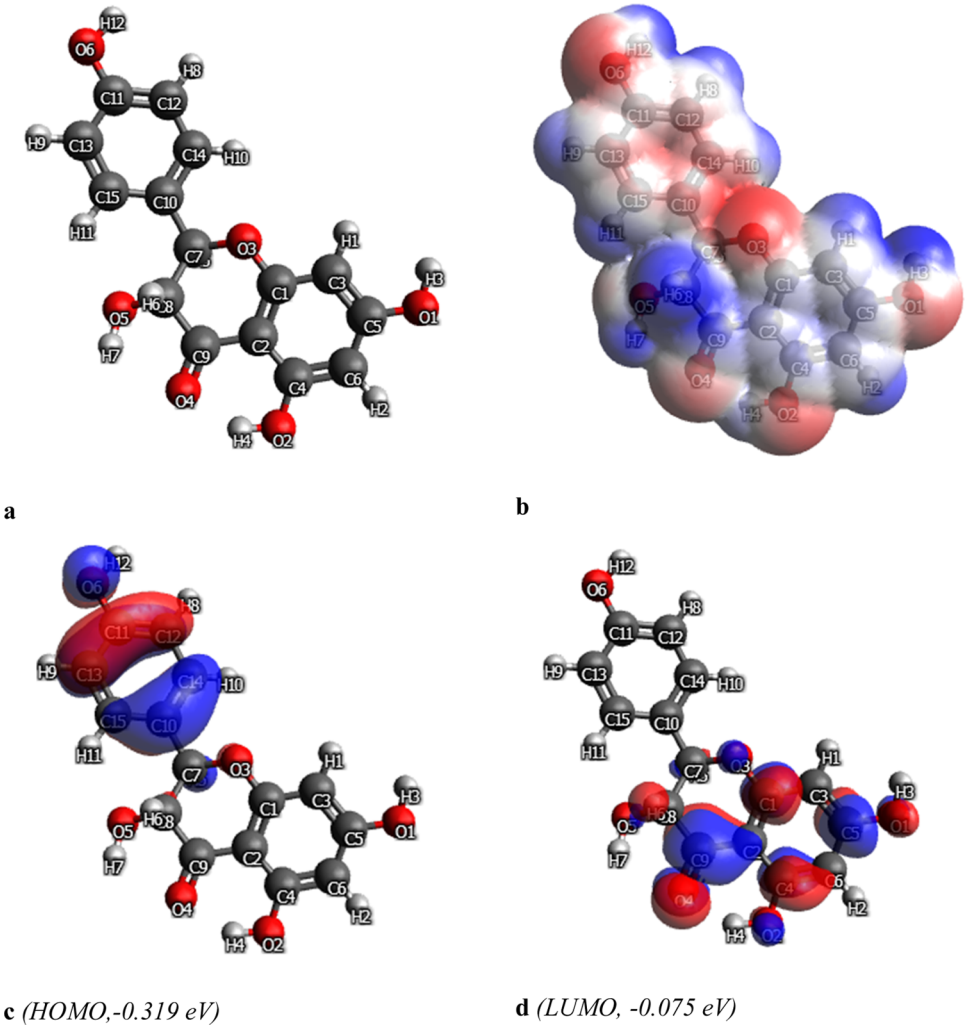

Figure 11. (a) Optimized structure and (b) MEP, (c) HOMO, and (d) LUMO structures of naringenin.

oglucinyl, pistaciaphenyl ether, and naringenin organic compounds are represented in Figures 9b, 10b, and 11b, respectively. The electrophilic and nucleophilic regions are indicated on these maps by the colors red and blue, respectively. This makes it generally clear that the pistiphloroglucinyl, pistaciaphenyl ether, and naringenin organic inhibitors contained many nucleophilic areas, confirming their favorable nucleophilic nature. The inhibition performances of pistiphloroglucinyl, pistaciaphenyl ethers, and naringenin increased in many nucleophilic regions. This is because the nucleophilic portions of the inhibitors have been adsorbed onto the steel surface. The aromatic rings and functional groups are centers of MEP regions.

3.7.4. Frontier Molecular Orbital (FMO) Investigations. FMO analysis estimated the electron distribution in HOMO and LUMO areas.[73−75] The resulting HOMOs of pistiphloroglucinyl, pistaciaphenyl ether, and naringenin organic compounds are represented in Figures 9c, 10c, and 11c, respectively. The results and discussion found are given below:

(i) The HOMO regions are mainly cited around C5−C11═C12 for pistiphloroglucinyl ether, C2−C1, C7−C8−C10, and C6−C5 for pistaciaphenyl ether, and C13−C11═C12 and C15−C10═C14 for naringenin organic compounds.

(ii) The electrons mainly occupied the HOMO regions, and as a result, the molecules are negatively charged.

(iii) The energies of HOMO orbitals for the selected compounds are as follows: pistaciaphenyl ether > pistiphloroglucinyl ether > naringenin organic compound. When compared to other corrosion inhibitors, pistaciaphenyl ether is more effective.

(iv) The bonding orbitals adsorb corrosion inhibitors on the steel surface.

(v) As a consequence of electrons being transferred to the unoccupied d-orbitals of Fe on the metal surface, this corrosion inhibitor can interact effectively with the metal surface, preventing corrosion.

On the other hand, LUMO regions were also found. The resulting LUMOs of pistiphloroglucinyl, pistaciaphenyl ethers, and naringenin organic compounds are represented in Figures 9d, 10d, and 11d, respectively. The results and discussion found are as follows:

(i) The LUMO areas show antibonding orbitals, which are more suitable for accepting electrons.

(ii) Some filled d-orbitals of Fe donate free electrons to antibonding orbitals of corrosion inhibitors (LUMO regions). Therefore, the LUMO regions promote chemical bond formation between the corrosion inhibitor and steel.[76,77]

https://doi.org/10.1021/acsomega.3c06824
ACS Omega 2024, 9, 7643−7657

3.7.5. Molecular Reactivity Investigations. The reactivity criteria of molecules of pistiphloroglucinyl, pistaciaphenyl ether, and naringenin organic compounds were evaluated by utilizing the energy difference ($\Delta E_{\mathrm{Inh}}^{\mathrm{DFT}}$) between the HOMO ($E_{\mathrm{HOMO(Inh)}}^{\mathrm{DFT}}$) and LUMO ($E_{\mathrm{LUMO(Inh)}}^{\mathrm{DFT}}$) according to eqs 9−18.[78−82] Table 6 presents the outcomes that were obtained.

Table 6. Theoretical Measurements of Corrosion Inhibitors (DFT, B3LYP, and 6-31G basis sets)

parameters	values (eV), pistiphloroglucinyl ether	values (eV), pistaciaphenyl ether	values (eV), naringenin
$E_{\mathrm{HOMO(Inh)}}^{\mathrm{DFT}}$	−0.201	−0.233	−0.319
$E_{\mathrm{LUMO(Inh)}}^{\mathrm{DFT}}$	0.005	−0.043	0.075
$\Delta E_{\mathrm{Inh}}^{\mathrm{DFT}}$	0.206	0.19	0.394
$\sigma_{\mathrm{Inh}}^{\mathrm{DFT}}$	9.4786	10.526	5.076
$\omega_{\mathrm{Inh}}^{\mathrm{DFT}}$	0.0478	0.1	0.0377
$\eta_{\mathrm{Inh}}^{\mathrm{DFT}}$	0.1055	0.095	0.197
$\chi_{\mathrm{Inh}}^{\mathrm{DFT}}$	0.1005	0.138	0.122
$I_{\mathrm{Inh}}^{\mathrm{DFT}}$	0.201	0.233	0.319
$A_{\mathrm{Inh}}^{\mathrm{DFT}}$	−0.005	0.043	−0.075
$\mu_{\mathrm{Inh}}^{\mathrm{DFT}}$	−0.1005	−0.138	−0.122
$\varepsilon_{\mathrm{Inh}}^{\mathrm{DFT}}$	20.92	10	26.52
$\Delta N_{\mathrm{Inh}}^{\mathrm{DFT}}$	32.7	36.1	17.45
$\psi_{\mathrm{Inh}}^{\mathrm{DFT}}$	16.35	18.06	8.72

As explored, the following main findings and discussions were found:

(i) The energy distinction between HOMO and LUMO demonstrates the nature of reactivity of inhibitors. It should be stressed that the obtained values of $\Delta E_{\mathrm{Inh}}^{\mathrm{DFT}}$ for pistiphloroglucinyl, pistaciaphenyl ether, and naringenin organic compounds were very low, confirming the high reactivity of these corrosion inhibitors. The order of values of $\Delta E_{\mathrm{Inh}}^{\mathrm{DFT}}$ is as follows: pistaciaphenyl ether > pistiphloroglucinyl ether > naringenin organic compound; this suggests that the pistaciaphenyl ether was more reactive than others. The main reason for this is the carboxyl functional groups and aromatic rings that promote the high reactivity of pistaciaphenyl ether. These results also confirm that molecules with higher reactivity are good corrosion inhibitors. Therefore, pistaciaphenyl ether is a better corrosion inhibitor than others.

(ii) The resulting values of chemical softness ($\sigma_{\mathrm{Inh}}^{\mathrm{DFT}}$) and chemical hardness ($\eta_{\mathrm{Inh}}^{\mathrm{DFT}}$) confirmed that the pistiphloroglucinyl, pistaciaphenyl ether, and naringenin organic compounds exhibit high chemical softness and lower hardness. Molecules with high chemical softness serve as good corrosion inhibitors. This means that the electrons are easily shared from the soft molecule to the metal surface.

(iii) The possible values of electronic nucleophilicity ($\varepsilon_{\mathrm{Inh}}^{\mathrm{DFT}}$), electron affinity ($\mathrm{A}_{\mathrm{Inh}}^{\mathrm{DFT}}$), global electrophilicity index ($\omega_{\mathrm{Inh}}^{\mathrm{DFT}}$), chemical potential ($\mu_{\mathrm{Inh}}^{\mathrm{DFT}}$), electronic negativity ($\chi_{\mathrm{Inh}}^{\mathrm{DFT}}$), and molecular ionization potential ($\mathrm{I}_{\mathrm{Inh}}^{\mathrm{DFT}}$) suggest that the pistiphloroglucinyl, pistaciaphenyl ether, and naringenin organic compounds are effective corrosion inhibitors.

(iv) Values of the electron fraction transfer ($\Delta \mathrm{N}_{\mathrm{Inh}}^{\mathrm{DFT}}$) (connected to Koopmans's theory) and the electronic fraction ($\psi_{\mathrm{Inh}}^{\mathrm{DFT}}$) revealed that the adsorption of pistiphloroglucinyl, pistaciaphenyl ether, and naringenin organic compounds onto the metal occur chemically by the transfer of the electrons.

$$\Delta E_{\mathrm{Inh}} = E_{\mathrm{LUMO(Inh)}} - E_{\mathrm{HOMO(Inh)}} \tag{9}$$

$$I_{\mathrm{Inh}} = -E_{\mathrm{HOMO(Inh)}} \tag{10}$$

$$A_{\mathrm{Inh}} = -E_{\mathrm{LUMO(Inh)}} \tag{11}$$

$$\eta_{\mathrm{Inh}} = \frac{1}{2(I_{\mathrm{Inh}} - A_{\mathrm{Inh}})} \tag{12}$$

$$\varepsilon_{\mathrm{Inh}} = \frac{1}{\omega_{\mathrm{Inh}}} \tag{13}$$

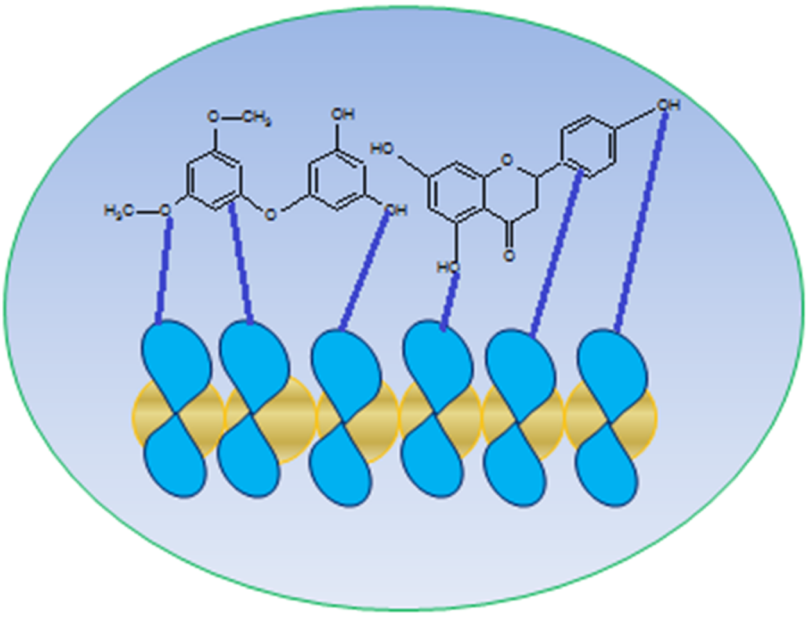

Figure 12. Phytochemical adsorption of P. integerrima on steel to form a protective coating.

https://doi.org/10.1021/acsomega.3c06824
ACS Omega 2024, 9, 7643−7657

$$-\mu_{Inh} = \chi_{Inh} = \frac{1}{2(I_{Inh} + A_{Inh})} \quad (14)$$

$$\omega_{Inh} = \frac{(\chi_{Inh})^2}{2\eta_{Inh}} \quad (15)$$

$$\sigma_{Inh} = \frac{1}{\eta} \quad (16)$$

$$\Delta N_{Inh} = \frac{(\chi_{Fe} - \chi_{Inh})}{2(\eta_{Fe} + \eta_{Inh})} \quad (17)$$

$$\psi_{Inh} = \frac{(\chi_{Fe} - \chi_{Inh})}{4(\eta_{Fe} + \eta_{Inh})} \quad (18)$$

where $\eta_{Fe} = 0$ eV mol^{-1} and $\chi_{Fe} = 7$ eV mol^{-1}.

3.8. Mechanism of Corrosion Inhibition by the *P. integerrima* Gall Extract on Mild Steel. During corrosion, oxidation takes place on the anode, and reduction takes place on the cathode.

$$Fe \rightarrow Fe^{2+} + 2^{e-}$$

$$2H^{+} + 2^{e-} \rightarrow H_2$$

A coordinate bond is formed when heteroatoms donate electrons to the metal orbital. The phytochemicals present in the *P. integerrima* extract can be used to reduce steel corrosion in 1 M sulfuric acid. In addition to double bonds, these phytochemicals have carbonyl, hydroxyl, and carboxylic acid functional groups. According to Figure 12, electrons in heteroatoms and multiple bonds in phytochemicals form coordinate bonds. Plant extracts block the active site by acting as inhibitors on the metal surface. As per the adsorption parameters, the value of ΔG°_{ads} indicates that the adsorption of the *P. integerrima* gall extract on the mild steel surface is physical in nature. Meanwhile, using DFT studies, it is observed that the *P. integerrima* gall extract is an inhibitor that adsorbs onto the metal surface by forming chemical bonds. In general, it can be concluded that both physical and chemical adsorption take place, and therefore, the extract can be considered to be a mixed-type corrosion inhibitor.

5. CONCLUSIONS

Many studies have been performed to assess the anticorrosive properties of the *P. integerrima* extract. The corrosion inhibition efficiency of the *P. integerrima* extract is determined by performing weight loss and electrochemical studies. According to EIS studies, we determined the maximum inhibition efficiency of 92.19% at an inhibitor concentration of 2000 mg L^{-1}. The obtained inhibition efficiency at various concentrations indicates that on increasing the inhibitor concentration, the corrosion rate decreases and inhibition efficiency increases. Surface morphological studies are in favor of the formation of a protective layer on the metal surface. Different phytochemicals found in the extract affect the potency of the inhibitor. The obtained results of DFT-based theoretical calculations confirmed that the order of values of corrosion efficiency is as follows: pistaciaphenyl ether > pistiphloroglucinyl ether > naringenin organic compound; this suggests that pistaciaphenyl ether was a more favored corrosion inhibitor than others. The reason for this is that the carboxyl functional groups as well as aromatic rings primarily promote the high reactivity of the pistaciaphenyl ether.

ASSOCIATED CONTENT

Supporting Information

The Supporting Information is available free of charge at https://pubs.acs.org/doi/10.1021/acsomega.3c06824.

Figure S1: Plant parts having different kinds of phytochemicals; Figure S2: Establishment of a protective layer on a steel surface in the presence of an inhibitor; Table S1: Different phytochemicals in plants; Table S2: Ability of some plants to suppress corrosion; Table S3: Phytochemicals of the *P. integerrima* gall extract (PDF)

AUTHOR INFORMATION

Corresponding Author

Akhil Saxena − *Department of Chemistry, Chandigarh University Mohali, Sahibzada Ajit Singh Nagar, Punjab 140413, India;* orcid.org/0000-0003-2501-5244; Email: akhil.uis@cumail.in

Authors

Jasdeep Kaur − *Department of Chemistry, Chandigarh University Mohali, Sahibzada Ajit Singh Nagar, Punjab 140413, India*

Hamad Almujibah − *Department of Civil Engineering, College of Engineering, Taif University, Taif City 21974, Saudi Arabia*

Mohammad Mahtab Alam − *Department of Basic Medical Sciences, College of Applied Medical Science, King Khalid University, Abha 61421, Saudi Arabia*

Abha Singh − *Department of Basic Sciences, College of Science and Theoretical Studies, Dammam-branch, Saudi Electronic University, Riyadh 11673, Saudi Arabia*

Dakeshwar Kumar Verma − *Department of Chemistry, Government Digvijay Autonomous Postgraduate College, Chhattisgarh 491441, India*

Elyor Berdimurodov − *New Uzbekistan University, Tashkent 100007, Uzbekistan; Medical School, Central Asian University, Tashkent 111221, Uzbekistan; Faculty of Chemistry, National University of Uzbekistan, Tashkent 100034, Uzbekistan*

Complete contact information is available at: https://pubs.acs.org/10.1021/acsomega.3c06824

Notes

The authors declare no competing financial interest.

ACKNOWLEDGMENTS

The authors express their gratitude to the Deanship of Scientific Research at King Khalid University for funding this work through the Large Research Groups Project under Grant No. RGP.2-504-44.

REFERENCES

(1) Schmitt, G.; Schütze, M.; Hays, G. F.; Burns, W.; Han, E.; Pourbaix, A.; Jacobson, G.*Global Needs for Knowledge Development in Materials Deterioration and Corrosion Control*, in cooperation with, Fed. Highw. Adm. FHWA-RD-01, 2009, pp 1-44.

(2) El-Hashemy, M. A.; Sallam, A. The inhibitive action of *Calendula officinalis* flower heads extract for mild steel corrosion in 1 M HCl solution. *J. Mater. Res. Technol.* **2020**, *9*, 13509−13523.

(3) Chung, I. M.; Malathy, R.; Priyadharshini, R.; Hemapriya, V.; Kim, S.; Prabakaran, M. Inhibition of mild steel corrosion using *Magnolia*

kobus extract in sulphuric acid medium. *Mater. Today Commun.* **2020**, *25*, No. 101687.
(4) Ahanotu, C. C.; Onyeachu, I. B.; Solomon, M. M.; Chikwe, I. S.; Chikwe, O. B.; Eziukwu, C. A. *Pterocarpus santalinoides* leaves extract as a sustainable and potent inhibitor for low carbon steel in a simulated pickling medium. *Sustainable Chem. Pharm.* **2020**, *15*, No. 100196.
(5) Saxena, A.; Thakura, K. K.; Bhardwaj, N. Electrochemilogycal studies and surface examination of low carbon steel by applying the extract of Musa acuminata. *Surf. Interfaces* **2020**, *18*, No. 100436.
(6) Zakaria, K.; Abbas, M.; Bedair, M. Herbal expired drug bearing glycosides and polysaccharides moieties as green and cost-effective oilfield corrosion inhibitor: Electrochemical and computational studies. *J. Mol. Liq.* **2022**, *352*, No. 118689.
(7) Haldhar, R.; Kim, S.; Prasad, D.; Bedair, M.; Bahadur, I.; Kaya, S.; Dagdag, O.; Guo, L. Papaver somniferum as an efficient corrosion inhibitor for iron alloy in acidic condition: DFT, MC simulation, LCMS and electrochemical studies. *J. Mol. Struct.* **2021**, *1242*, No. 130822.
(8) Parthipan, P.; Elumalai, P.; Narenkumar, J.; Machuca, L.; Murugan, K.; Karthikeyan, O.; Rajasekar, A. Allium sativum (garlic extract) as a green corrosion inhibitor with biocidal properties for the control of MIC in carbon steel and stainless steel in oilfield environments. *Int. Biodeterior. Biodegrad.* **2018**, *132*, 66−73.
(9) Saxena, A.; Prasad, D.; Haldhar, R.; Singh, G.; Kumar, A. Use of *Sida cordifolia* Extract as Green Inhibitor for Mild Steel in 0.5M H_2SO_4. *J. Environ. Chem. Eng.* **2018**, *6*, 694−700.
(10) Saxena, A.; Prasad, D.; Haldhar, R.; Singh, G.; Kumar, A. Use of *Saraca ashoka* extract as green corrosion inhibitor for mild steel in 0.5 M H2SO4. *J. Mol. Liq.* **2018**, *258*, 89−97.
(11) Saxena, A.; Prasad, D.; Haldhar, R. Investigation of corrosion inhibition effect and adsorption activities of Cuscuta reflexa extract for mild steel in 0.5 M H_2SO_4. *Bioelectrochemistry* **2018**, *124*, 156−16.
(12) Haldhar, R.; Prasad, D.; Saxena, A. Armoracia rusticana as sustainable and eco-friendly corrosion inhibitor for mild steel in 0.5M sulphuric acid: Experimental and theoretical investigations. *J. Environ. Chem. Eng.* **2018**, *6*, 5230−5238.
(13) Haldhar, R.; Prasad, D.; Saxena, A. Myristica fragrans extract as an eco-friendly corrosion inhibitor for mild steel in 0.5 M H2SO4 solution. *J. Environ. Chem. Eng.* **2018**, *6*, 2290−2301.
(14) Alibakhshi, E.; Ramezanzadeh, M.; Bahlakeh, G.; Ramezanzadeh, B.; Mahdavian, M.; Motamedi, M. Glycyrrhiza glabra leaves extract as a green corrosion inhibitor for mild steel in 1 M hydrochloric acid solution: Experimental, molecular dynamics, Monte Carlo and quantum mechanics study. *J. Mol. Liq.* **2018**, *255*, 185−198.
(15) Satapathy, A.; Gunasekaran, G.; Sahoo, S.; Amit, K.; Rodrigues, P. Corrosion inhibition by Justicia gendarussa plant extract in hydrochloric acid solution. *Corros. Sci.* **2009**, *51*, 2848−2856.
(16) Chauhan, L.; Gunasekaran, G. Corrosion inhibition of mild steel by plant extract in dilute HCl medium. *Corros. Sci.* **2007**, *49*, 1143−1161.
(17) El-Etre, A. Khillah extract as inhibitor for acid corrosion of SX 316 steel. *Appl. Surf. Sci.* **2006**, *252*, 8521−8525.
(18) Oguzie, E. E. Studies on the inhibitive effect of Occimum viridis extract on the acid corrosion of mild steel. *Mater. Chem. Phys.* **2006**, *99*, 441−446.
(19) El-Etre, A.; Abdallah, M.; El-Tantawy, Z. Corrosion inhibition of some metals using lawsonia extract. *corros. Sci.* **2005**, *47* (X), 385−395.
(20) Lebrini, M.; Robert, F.; Lecante, A.; Roos. Corrosion inhibition of C38 steel in 1 M hydrochloric acid medium by alkaloids extract from *Oxandra asbeckii* plant. *Corros. Sci.* **2011**, *53*, 687−695.
(21) Bhawsar, J.; Ain, Pk.; Jain, P. Experimental and computational studies of *Nicotiana tabacum* leaves extract as green corrosion inhibitor for mild steel in acidic medium. *Alexandria Eng. J.* **2015**, *54*, 769−774.
(22) Ngouné, B.; Pengou, M.; Nouteza, A.; Nanseu-Njiki, C.; Ngameni, E. Performances of Alkaloid Extract from Rauvolfia macrophylla Stapf toward Corrosion Inhibition of C38 Steel in Acidic Media. *ACS Omega* **2019**, *4*, 9081−9091.
(23) Prabakaran, M.; Hemapriya, S.; Kim, V.; Chung, I. Evaluation of polyphenol composition and anti-corrosion properties of *Cryptostegia grandiflora* plant extract on mild steel in acidic medium. *J. Indust. Eng. Chem.* **2016**, *37*, 2016.
(24) Hassan, K. H.; Khadom A, A.; Kurshed, N. *Citrus aurantium* leaves extracts as a sustainable corrosion inhibitor of mild steel in sulfuric acid. *S. Afr. J. Chem. Eng.* **2016**, *22*, 1−5.
(25) Dehghani, A.; Bahlakeha, G.; Ramezanzadeh, B. A detailed electrochemical/theoretical exploration of the aqueous *Chinese gooseberry* fruit shell extract as a green and cheap corrosion inhibitor for mild steel in acidic solution. *J. Mol. Liq.* **2019**, *282*, 366−384.
(26) Dehghani, A.; Bahlakeha, G.; Ramezanzadehb, B.; Ramezanzadeh, M. Potential of *Borage* flower aqueous extract as an environmentally sustainable corrosion inhibitor for acid corrosion of mild steel: Electrochemical and theoretical studies. *J. Mol. Liq.* **2019**, *277*, 895−911.
(27) Benarioua, M.; Mihi, A.; Bouzeghaia, N.; Naoun. Mild steel corrosion inhibition by Parsley (Petroselium Sativum) extract in acidic media. *Egypt. J. Pet.* **2019**, *28*, 155−159.
(28) Muthukrishnan, P.; Jeyaprabha, B.; Prakash, P. Adsorption and corrosion inhibiting behavior of *Lannea coromandelica* leaf extract on mild steel corrosion. *Arabian J. Chem.* **2013**, S2343−S2354.
(29) Mehdipour, M.; Ramezanzadeh, B.; Arman, S. Electrochemical noise investigation of Aloe plant extract as green inhibitor on the corrosion of stainless steel in 1 M H_2SO_4. *J. Indust. Eng. Chem.* **2015**, *21*, 318−327.
(30) Uwah, I.; Okafor, P.; Ebiekpe, V. Inhibitive action of ethanol extracts from *Nauclea latifolia* on the corrosion of mild steel in H_2SO_4 solutions and their adsorption characteristics. *Arabian J. Chem.* **2013**, *6*, 253−352.
(31) Bagga, M. K.; Gadi, R.; Yadav, O.; Kumar, R.; Chopra, R.; Singh, G. Investigation of phytochemical components and corrosion inhibition property of Ficus racemosa stem extract on mild steel in H2SO4 medium. *J. Environ. Chem. Eng.* **2016**, *4*, 4699−4707.
(32) Haldhar, R.; Prasad, D.; Mandal, N.; Benhiba, F.; Bahadur, I.; Dagdag, O. Anticorrosive properties of a green and sustainable inhibitor from leaves extract of Cannabis sativa plant: Experimental and theoretical approach. *Colloids Surf., A* **2021**, *614*, No. 126211.
(33) Patel, N.; Šnita, D. Ethanol extracts of Hemidesmus indicus leaves as eco-friendly inhibitor of mild steel corrosion in H_2SO_4 medium. **2014**, 1747 1754.
(34) Umoren, S.; Obot, I.; Israel, A.; Asuquo, P.; Solomon, M.; Eduok, U.; Udoh, A. Inhibition of mild steel corrosion in acidic medium using coconut coir dust extracted from water and methanol as solvents. *J. Ind. Eng. Chem.* **2014**, *20*, 3612−3622.
(35) Singh, M. A green Approach: A corrosion inhibition of mild steel by adhatoda vasica plant extract in 0.5 M H2SO4. *J. Mater. Environ. Sci.* **2013**, *4*, 119−126.
(36) Dehghani, A.; Bahlakeh, G.; Ramezanzadeh, B.; Ramezanzadeh, M. A combined experimental and theoretical study of green corrosion inhibition of mild steel in HCl solution by aqueous Citrullus lanatus fruit (CLF) extract. *J. Mol. Liq.* **2019**, *279*, 603−624.
(37) Dehghani, A.; Bahlakeh, G.; Ramezanzadeh, B. Green Eucalyptus leaf extract: A potent source of bio-active corrosion inhibitors for mild steel. *Bioelectrochemistry* **2019**, *130*, No. 107339.
(38) Wang, Y.; Qiang, Y.; Zhi, H.; Ran, B.; Zhang, D. Evaluating the synergistic effect of maple leaves extract and iodide ions on corrosion inhibition of Q235 steel in H2SO4 solution. *J. Ind. Eng. Chem.* **2023**, *117*, 422−33.
(39) Yao, X.; Qiang, Y.; Guo, L.; Xu, Q.; Wen, L.; Jin, Y. Renewable low-cost brassica rapa subsp. Extract for protection of Q235 steel in H2SO4 medium: Experimental and modeling studies. *J. Ind. Eng. Chem.* **2022**, *114*, 427−37.
(40) Bedair, M.; Metwally, M.; Soliman, S.; Al-Sabagh, A.; Salem, A.; Mohamed, T. EXTRACTS OF MINT AND TEA AS GREEN CORROSION INHIBITORS FOR MILD STEEL IN HYDROCHLORIC ACID SOLUTION. *Al-Azhar Bull. Sci.* **2015**, *26*, 1−14.
(41) Hassan, A.; Heakal, B.; Younis, A.; Bedair, M.; El - Billy, M.; Mohamed, M. Synthesis of some triazole Schiff base derivatives and their metal complexes under Microwave irradiation and evaluation of their corrosion inhibition and biological activity. *Egypt. J. Chem.* **2019**.

https://doi.org/10.1021/acsomega.3c06824
ACS Omega 2024, 9, 7643−7657

(42) Raja, P. B.; Qureshi, A.; Rahim, A.; Osman, H.; Awang, K. Neolamarckia cadamba alkaloids as eco-friendly corrosion inhibitors for mild steel in 1M HCl media. *Corros. Sci.* **2013**, *69*, 292−301.
(43) Lgaz, H.; Salghi, R.; Jodeh, S.; Hammouti, B. Effect of clozapine on inhibition of mild steel corrosion in 1.0 M HCl medium. *J. Mol. Liq.* **2017**, *225*, 271−280.
(44) Majeed, M.; Yousif, Q.; Bedair, M. Study of the Corrosion of Nickel−Chromium Alloy in an Acidic Solution Protected by Nickel Nanoparticles. *ACS Omega* **2022**, 729850−29857.
(45) Elaryian, H. M.; Bedair, M.; Bedair, A.; Aboushahba, R.; Fouda, A. Synthesis, characterization of novel coumarin dyes as corrosion inhibitors for mild steel in acidic environment: Experimental, theoretical, and biological studies. *J. Mol. Liq.* **2022**, *346*, No. 118310.
(46) Ismail, A. M.; Mohamed, E.; Marghany, M.; Motaal, V.; Abdel-Farid, V. I.; Sayed, M. E. Preliminary phytochemical screening, plant growth inhibition and antimicrobial activity studies of Faidherbia albida legume extracts. *J. Saudi Soc. Agric. Sci.* **2016**, *15*, 112−117.
(47) Alqethami, A.; Aldhebiani, A. Medicinal plants used in Jeddah, Saudi Arabia: Phytochemical screening. *Saudi J. Biol. Sci.* **2021**, *28*, 805−812.
(48) Kumar, J.; Kaur, A.; Narang, P. Phytochemical screening and metal binding studies on floral extract of Solanum nigrum. *Mater. Today: Proc.* **2020**, *26*, 3332−3336.
(49) El-Sabbah, M.; Bedair, M.; Abbas, M.; Fahmy, A.; Hassaballa, S.; Moustafa, A. Synergistic Effect between Natural Honey and 0.1 M KI as Green Corrosion Inhibitor for Steel in Acid Medium. *Zeitsch. Phys. Chem.* **2019**, *233*, 627−649.
(50) Dewangan, Y.; Verma, D.; Berdimurodov, E.; Haldhar, R.; Dagdag, O.; Tripathi, M.; Mishra, V.; Kumar, P. N-hydroxypyrazine-2-carboxamide as a new and green corrosion inhibitor for mild steel in acidic medium: experimental, surface morphological and theoretical approach. *J. Adhes. Sci. Technol.* **2022**, *36*, 1−21.
(51) Berdimurodov, E.; Kholikov, A.; Akbarov, K.; Guo, L.; Kaya, S.; Verma, D. K.; Rbaa, M.; Dagdag, O. Novel glycoluril pharmaceutically active compound as a green corrosion inhibitor for the oil and gas industry. *J. Electroanal. Chem.* **2022**, *907*, No. 116055.
(52) Dagdag, O.; Haldhar, R.; Kim, S.-C.; Guo, L.; El Gouri, M.; Berdimurodov, E.; Hamed, O.; Jodeh, S.; Akpan, E. D.; Ebenso, E. E. Recent progress in epoxy resins as corrosion inhibitors: design and performance. *J. Adhes. Sci. Technol.* **2022**, 1−22.
(53) Berdimurodov, E.; Kholikov, A.; Akbarov, K.; Guo, L.; Abdullah, A. M.; Elik, M. A gossypol derivative as an efficient corrosion inhibitor for St2 steel in 1 M HCl + 1 M KCl: An experimental and theoretical investigation. *J. Mol. Liq.* **2021**, *328*, No. 115475.
(54) Barca, G. M. J.; Bertoni, C.; Carrington, L.; Datta, D.; De Silva, N.; Deustua, J. E.; Fedorov, D. G.; Gour, J. R.; Gunina, A. O.; Guidez, E.; et al. Recent developments in the general atomic and molecular electronic structure system. *J. Chem. Phys.* **2020**, *152*, No. 154102.
(55) Schmidt, M. W.; Baldridge, K. K.; Boatz, J. A.; Elbert, S. T.; Gordon, M. S.; Jensen, J. H.; Koseki, S.; Matsunaga, N.; Nguyen, K. A.; Su, S.; et al. General atomic and molecular electronic structure system. *J. Comput. Chem.* **1993**, *14*, 1347−1363.
(56) Becke, A. D. Density-functional thermochemistry. III. The role of exact exchange. *J, Chem. Phys.* **1993**, *98* (n.d.), 5648.
(57) Lee, C.; Yang, W.; Parr, R. G. Development of the Colle-Salvetti correlation-energy formula into a functional of the electron density. *Phys. Rev. B* **1988**, *37*, 785.
(58) Hanwell, M. D.; Curtis, D. E.; Lonie, D. C.; Vandermeersch, T.; Zurek, E.; Hutchison, G. R. Avogadro: an advanced semantic chemical editor, visualization, and analysis platform. *J. Cheminform.* **2012**, *4*, 1−17.
(59) A. an open-source molecular builder and visualization tool. V. 1. X. http://avogadro.cc/.
(60) Bedair, M.; Alosaimi, E.; Melhi, S. A study of the inhibitive effect for corrosion of steel in 1.0 M HCl using a new nonionic surfactant based on coumarin moiety: chemical, electrochemical and quantum mechanics calculations. *J. Adhes. Sci. Technol.* **2021**, 1−31.
(61) Abdelsalam, M. M.; Bedair, M.; Hassan, A.; Heakal, B.; Younis, A.; Elbialy, Z.; Badawy, M.; Fawzy, H.; Fareed, S. Green synthesis, electrochemical, and DFT studies on the corrosion inhibition of steel by some novel triazole Schiff base derivatives in hydrochloric acid solution. *Arab. J. Chem.* **2022**, *15*, No. 103491.
(62) Shabani-Nooshabadi, M.; Ghandchi, M. Santolina chamaecyparissus extract as a natural source inhibitor for 304 stainless steel corrosion in 3.5% NaCl. *J. Ind. Eng. Chem.***2015** *31* 231−237. .
(63) Ferreira, E.; Giacomelli, C.; Giacomelli, F.; Spinelli, A. Evaluation of the inhibitor effect of L-ascorbic acid on the corrosion of low alloy steel. *Mater. Chem. Phys.* **2004**, *83*, 129−134.
(64) Gebril, M. A.; Bedair, M.; Soliman, S.; Bakr, F.; Mohamed M, M. Experimental and computational studies of the influence of non-ionic surfactants with coumarin moiety as corrosion inhibitors for carbon steel in 1.0 M HCl. *J. Mol. Liq.* **2022**, *349*, No. 118445.
(65) Mostafa, M.; Ashmawy, A.; Reheim, M.; Bedair, M.; Abuelela, A. Molecular structure aspects and molecular reactivity of some triazole derivatives for corrosion inhibition of aluminum in 1 M HCl solution. *J. Mol. Struct.* **2021**, *1236*, No. 130292.
(66) Berdimurodov, E.; Kholikov, A.; Akbarov, K.; Guo, L. Experimental and theoretical assessment of new and eco−friendly thioglycoluril derivative as an effective corrosion inhibitor of St2 steel in the aggressive hydrochloric acid with sulfate ions. *J. Mol. Liq.* **2021**, *335*, No. 116168.
(67) Shahmoradi, A.; Ranjbarghanei, M.; Javidparvar, A.; Guo, L.; Berdimurodov, E.; Ramezanzadeh, B. Theoretical and surface/electrochemical investigations of walnut fruit green husk extract as effective inhibitor for mild-steel corrosion in 1M HCl electrolyte. *J. Mol. Liq.* **2021**, *338*, No. 116550.
(68) Haldhar, R.; Kim, S.; Berdimurodov, E.; Verma, D.; Hussain, C. (2021) Corrosion Inhibitors: Industrial Applications and Commercialization, in: *Sustain. Corros. Inhib. II Synth. Des. Pract. Appl.*; American Chemical Society, 210−219. .
(69) Dagdag, O.; Berisha, A.; Mehmeti, V.; Haldhar, R.; Berdimurodov, E.; Hamed, O.; Jodeh, S.; Lgaz, H.; Sherif, E.; Ebenso, E. Epoxy coating as effective anti-corrosive polymeric material for aluminum alloys: Formulation, electrochemical and computational approaches. *J. Mol. Liq.* **2022**, *346*, No. 117886.
(70) Berdimurodov, E.; Kholikov, A.; Akbarov, K.; Guo, L.; Kaya, S.; Katin, K.; Verma, D.; Rbaa, M.; Dagdag, O. Novel cucurbit[6]uril-based [3]rotaxane supramolecular ionic liquid as a green and excellent corrosion inhibitor for the chemical industry. *Colloids Surf., A* **2022**, *633*, No. 127837.
(71) Berdimurodov, E.; Kholikov, A.; Akbarov, K.; Guo, L.; Kaya, S.; Verma, D.; Rbaa, M.; O Dagdag, O. New and Green Corrosion Inhibitor Based on New Imidazole Derivate for Carbon Steel in 1 M Hcl Medium: Experimental and Theoretical Analyses. *Int. J. Eng. Res. Africa* **2022**, *58*, 11−44.
(72) Berdimurodov, E.; Guo, L.; Kholikov, A.; Akbarov, K.; Zhu, M. MOFs-Based Corrosion Inhibitors. *Supramol. Chem. Corros. Biofouling Prot.*, CRC Press: 2022; pp 287−305.
(73) Bahgat Radwan, A.; Mannah, C.; Sliem, M.; Al-Qahtani, N.; Okonkwo, P.; Berdimurodov, E.; Mohamed, A.; Abdullah, A. Electrospun highly corrosion-resistant polystyrene−nickel oxide superhydrophobic nanocomposite coating. *J. Appl. Electrochem.* **2021**, *51*, 1605−1618.
(74) Berdimurodov, E.; Kholikov, A.; Akbarov; Guo, L.; Kaya, S.; Katin, K.; Verma, D.; Rbaa, M.; Dagdag, O.; Haldhar, R. Novel bromide−cucurbit[7]uril supramolecular ionic liquid as a green corrosion inhibitor for the oil and gas industry. *J. Electroanal. Chem.* **2021**, *901*, No. 115794.
(75) Berdimurodov, E.; Verma, C.; Berdimuradov, K.; Quraishi, M.; Kholikov, A.; Akbarov, K.; Umirov, N.; Borikhonov, B. 8−Hydroxyquinoline is key to the development of corrosion inhibitors: An advanced review. *Inorg. Chem. Commun.* **2022**, *144*, No. 109839.
(76) Berdimurodov, E.; Eliboyev, I.; Berdimuradov, K.; Kholikov, A.; Akbarov, K.; Dagdag, O.; Rbaa, M.; El Ibrahimi, B.; Ibrahimi, B.; Verma, D.; Haldhar, R. Green β-cyclodextrin-based corrosion inhibitors: Recent developments, innovations and future opportunities. *Carbohydr. Polym.* **2022**, *292*, No. 119719.

https://doi.org/10.1021/acsomega.3c06824
ACS Omega 2024, 9, 7643−7657

(77) Zhu, M.; Guo, L.; He, Z.; Z Marzouki, H.; Marzouki, R.; Zhang, R.; Zhang, R.; Berdimurodov, E. Insights into the newly synthesized N-doped carbon dots for Q235 steel corrosion retardation in acidizing media: A detailed multidimensional study. *J. Colloid Interface Sci.* **2022**, *608*, 2039−2049.
(78) Berdimurodov, E.; Verma, D. K.; Kholikov, A.; Akbarov, K.; Guo, L. The recent development of carbon dots as powerful green corrosion inhibitors: A prospective review. *J. Mol. Liq.* **2022**, *349*, No. 118124.
(79) Verma, D. K.; Kazi, M.; Alqahtani, M. S.; Syed, R.; Berdimurodov, E.; Kaya, S.; Salim, R.; Asatkar, A.; Haldhar, R. N−hydroxybenzothioamide derivatives as green and efficient corrosion inhibitors for mild steel: Experimental, DFT and MC simulation approach. *J. Mol. Struct.* **2021**, *1241*, No. 130648.
(80) Vashishth, P.; Bairagi, H.; Narang, R.; Shukla, S.; Mangla, B. Thermodynamic and electrochemical investigation of inhibition efficiency of green corrosion inhibitor and its comparison with synthetic dyes on MS in acidic medium. *J. Mol. Liq.* **2022**, *365*, No. 120042.
(81) Qiang, Y.; Zhi, H.; Guo, L.; Fu, A.; Xiang, T.; Jin, Y. Experimental and molecular modeling studies of multi-active tetrazole derivative bearing sulfur linker for protecting steel from corrosion. *J. Mol. Liq.* **2022**, *351*, No. 118638.
(82) Qiang, Y.; Guo, L.; Li, H.; Lan, X. Fabrication of environmentally friendly Losartan potassium film for corrosion inhibition of mild steel in HCl medium. *Chem. Eng. J.* **2021**, *406*, No. 126863.

https://doi.org/10.1021/acsomega.3c06824
ACS Omega 2024, 9, 7643−7657